The Journal of Experimental Biology 203, 161–170 (2000)
Printed in Great Britain © The Company of Biologists Limited 2000
JEB2346

ANALYSIS OF THE MEMBRANE DOMAIN OF THE GASTRIC H^+/K^+-ATPase

KEITH MUNSON, NILS LAMBRECHT, JAI MOO SHIN AND GEORGE SACHS*
University of California at Los Angeles and Wadsworth VA Hospital, Los Angeles, CA 90073, USA
*Author for correspondence (e-mail: gsachs@ucla.edu)

Accepted 18 October; published on WWW 13 December 1999

Summary

A structure of the catalytic or alpha subunit of the H^+/K^+-ATPase, with ten transmembrane segments, and of the beta subunit, with a single such segment, was established using a combination of tryptic cleavage and peptide sequencing and *in vitro* translation. Sites at which covalent ligands bind to external surfaces were also defined by cleavage, separation and sequencing. Cys813 was found to be the common covalent binding site for all the substituted pyridyl methylsulfinyl benzimidazoles. The binding region of a K^+-competitive reagent, the 1,2α-imidazo-pyridine SCH 28080, was defined by the kinetic effects of site-specific mutations. Amino acids substitutions in membrane-spanning segments M1, M3, M4 and M6 were found to influence the apparent inhibitor constant, K_i, to varying degrees, some having a large effect, some a moderate effect and some a slight effect, whereas some mutations had no effect. We interpret changes in K_i without effects on the apparent Michaelis constant, K_m, as affecting SCH 28080 binding only. Mutation of Cys813 significantly affected the K_i for SCH 28080, explaining the prevention of benzimidazole inhibition by the imidazo-pyridine.

A model of the alpha subunit was constructed with a vestibule on the luminal surface of the pump bounded by M1–M6 and containing the SCH 28080 binding region. The cation binding site is suggested to be more towards the cytoplasmic face of the enzyme's membrane domain. This model predicts the membrane peptide associations for the catalytic subunit. Biochemical and yeast two-hybrid methods place the beta subunit in association with M8, whereas similar methods place M5/6 in proximity to M9/10. These results, when combined with analysis of the two-dimensional crystals of the sarcoplasmic reticular Ca^{2+} and *Neurospora crassa* H^+-ATPases, provide the basis for a tentative model of the arrangement of the six core segments of the gastric H^+/K^+-ATPase.

Key words: H^+/K^+-ATPase, structure, membrane domain.

Introduction

An ion pump gets its name from its ability to move ions uphill, or against a concentration gradient, and requiring input of energy across a membrane that is an asymmetric phospholipid bilayer. The mechanical pumps created by man, such as those powered by rotary pistons, linear motors or other devices, may reflect the biological choice for such devices. A pump, biological or mechanical, must derive energy from some source. A biological pump derives energy from the breakdown of substrates, such as by oxidation or hydrolysis, from absorption of light or from ATP. These scalar processes are converted to the vectorial property of transport by the orientation of the protein across a membrane bilayer, whence conformational changes induced by energization in the protein are translated into transmembrane ion motion either with rotation, as in the F_1F_o or V-ATPases, or by membrane helix tilt, as in rhodopsins or P-ATPases.

We are fast approaching what seemed impossible 40 years ago when the proteins responsible for ion pumping began to be discovered, the ability to describe a pump in molecular detail, that is to say not only in terms of its linear amino acid sequence but in terms of the arrangement of this sequence in three dimensions and of the changes that take place in this structure to enable ion pumping.

Even with diversity of pumping mechanisms, there will be general structural features that will allow immediate recognition of an ion pump. These features include the presence of membrane-embedded segments of the pump with protein disposed to varying degrees on either side of the membrane. Of these membrane-embedded segments, some will be in close contact with the hydrocarbon phase of the phospholipid, some more in contact with each other, providing the possibility of translational or rotational motion, the former being applied by single-unit pumps, the latter by multi-subunit pumps with distinct peptides for the cytoplasmic and membrane domains. The cytoplasmic domain of an ATP-driven pump will contain signature sequences for ATP or ADP and inorganic phosphate (P_i) binding, perhaps for phosphorylation, binding sites for Mg^{2+} and other as yet undefined binding sites. With our current state of knowledge, the nature of the ion transported is not obvious either from the sequence or from the arrangement of the membrane segments. A general rule seems to be that carboxylic acids are often

implicated in the transport of small cations. This is less clear for the transition-metal ion pumps.

Ion-translocating ATPases can be classified into F_1-ATPases, V-ATPases, P-ATPases and APL- (aminophospholipid-transporting) ATPases (Sachs, 1998). Of these, the first two are multi-subunit pumps in which the energy-transducing or ATPase sector is chemically separate from the ion-translocating sector, whereas the P-type ATPases combine these two functions into a single protein. There is a clear mechanistic split between these two types of pump, one using rotational energy in the membrane domain for ion transport, the other altering membrane helix interactions to enable active ion transport. The P-type ATPases belong to the latter type. In the multi-subunit pumps, only H^+ or Na^+ have been shown to be transported. Perhaps the evolutionary divergence that occurred to form single-subunit pumps was driven by the advantage conferred by active transport of a variety of cations. The Kdp-ATPase, a protein with eight membrane-spanning segments, is used by a variety of bacteria to import K^+ and, although composed of three subunits, may be the ancestor of single-subunit ATP-driven pumps (Gassel et al., 1998).

As a paradigm for the analysis of structure/transport coupling of a P-ATPase, we shall discuss the gastric H^+/K^+-ATPase, a member of the P_2-type ATPase family, namely ATPases transporting alkali cations and other small cations such as Ca^{2+} and Mg^{2+}, to contrast it with the P_1-type ATPase family, which transports transition-metal ions. These single-subunit pumps are polytopic integral membrane proteins, consisting of a relatively large cytoplasmic domain, a multiple-segment membrane domain and a smaller external or luminal domain. The small ion pumps have 10 membrane-inserted sequences (Serrano, 1988), whereas the transition-metal pumps have eight (Bayle et al., 1998; Melchers et al., 1996). In both cases, two adjacent pairs of membrane-inserted segments are separated by large cytoplasmic loops, the second of which contains the ATP-binding and phosphorylation domains. In the case of the P_1-ATPases, these loops are between membrane-spanning segments M5/6 and M7/8, whereas in the P_2-ATPases these loops are between M2/3 and M4/5.

At low resolution, crystals of the enzyme appear to show a groove in the cytoplasmic domain, presumably containing the ATP-binding domain and access for the ion to the membrane domain. Changes of conformation in the cytoplasmic domain are transmitted to the membrane helices, altering their interactions to allow the ion to pass across the membrane. The focus of this review of the gastric ATPase is therefore on the membrane domain and possible regions of transmembrane passage of either H^+ or K^+.

Gastric H^+/K^+-ATPase

General properties

The gastric H^+/K^+-ATPase is a member of the P_2-type ATPase family and is responsible for gastric acid secretion. The enzyme undergoes a cycle of phosphorylation and dephosphorylation coupled to the outward movement of H^+ and the inward movement of K^+ in a net electroneutral fashion. Earlier research on these ATPases, prior to the availability of cDNA-derived sequences, concentrated on the coupling between transport and catalysis, and vital concepts were derived from these studies, particularly those relating to phosphorylation/dephosphorylation and ion transport (Sachs et al., 1976; Forte et al., 1974).

The enzyme transports ions in either direction as a function of conformational changes in the cytoplasmic domain. The data derived for these ATPases seem all to conform to a general model in which the binding of ATP and the outward-transported ion results in phosphorylation of the pump at a particular region of the protein, the phosphorylation signature sequence, DKTGTLT, where the aspartyl at position 386 is phosphorylated in the case of the gastric ATPase (Walderhaug et al., 1985). When this phosphorylation occurs, the inward-facing ion-binding site with high affinity is altered to form an outward-facing ion-binding site of lower affinity. This transition is generally referred to as the E_1 to E_2 transition, these numerals implying a major conformational change. Between the inward E_1 and outward E_2 ion-binding states, yet a third ion-binding site state has been inferred, in which the ion is shielded from either side of the membrane, the occluded state.

This state can be defined experimentally in terms of ion binding. Occlusion can be demonstrated even after cleavage of the connections between the cytoplasm and the membrane segments. Hence, this property resides within the membrane domain of the pump. The first evidence for this conformation was deduced by comparing the rate of Na^+/K^+-ATPase activity in the presence of different dephosphorylating cations (K^+, Rb^+, NH_4^+) where the concentrations of these cations had been set to give equal rates of dephosphorylation. The ATPase activities were different, showing that the rate-limiting step was due to release of the counter-transported cation by binding of ATP, and this was thought to be the occluded state (Beauge and Glynn, 1979). Direct evidence for this state was then obtained by measuring cation binding to enzymes such as the Na^+/K^+-, Ca^{2+}- and H^+/K^+-ATPases (Esmann, 1985; Vilsen and Andersen, 1986; Rabon et al., 1993).

With release of the ion to the outside, the counterion binds, enabling dephosphorylation of the E_2–P state of the enzyme, formation of the E_2 state of the bound counterion site or state and then transition back to the E_1 state, with cytoplasmic release of the inwardly transported ion. As in the forward reaction, the ion site transits between the E_2 and E_1 states through an occluded form. It seems likely that the transport reactions not only occur across the transmembrane domain but are also initiated on either side of the membrane within close proximity to the membrane domain. Fig. 1 illustrates the general kinetic scheme developed for a counter-transport pump such as the mammalian alkali-cation P-type ATPases, as applied in particular to the gastric H^+/K^+-ATPase.

General structural features

In contrast to the monomeric H^+-ATPases of yeast and other

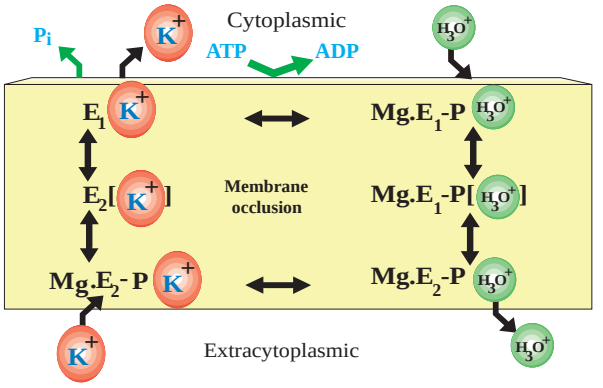

Fig. 1. The Post–Albers scheme for transport catalysis coupling as applied to the gastric H^+/K^+-ATPase. This enzyme probably transports H_3O^+ (not H^+, since Na^+ can substitute at high pH; Polvani et al., 1989), which is moved out of the cell as shown on the right-hand side of the figure. After release of H_3O^+, K^+ can bind and be transported inwards *via* the occluded, dephosphorylated state as shown on the left-hand side of the figure. E_1, inward ion-binding state; E_2, outward ion-binding state; P_i, inorganic phosphate.

fungi and the Ca^{2+}- or Mg^{2+}-ATPases, the gastric ATPase is composed of two subunits, the alpha subunit, which contains the signature phosphorylation sequence within the sequence of 1033 amino acid residues, and the beta subunit, which has six or seven N-linked glycosylation sites in its sequence of 291 amino acid residues. As such, it is a representative of a subfamily of ATPases that have two such subunits, namely the Na^+/K^+ P_2-ATPases and the colonic and skin K^+ P_2-ATPase subfamily, which also have two subunits. The function of these beta subunits is not clear, but the beta subunit appears to be required at least for assembly of the catalytic subunit (Geering, 1991), but chemical alteration of the beta subunit affects ATPase activity as well (Chow et al., 1992). It is of interest that the pumps that have a beta subunit are counter-transport pumps transporting K^+ or its surrogates inwards. Perhaps the beta subunit has a function in maintaining the structure of the alpha subunit to enable effective binding of the counter-cation to the outside face of the alpha subunit in the region of M8, where there is strong association between the beta and alpha subunits (Hasler et al., 1998).

As for all these P_2-ATPases, the membrane domain of the alpha subunit contains 10 membrane-inserted segments, whereas the P_1-ATPases have eight such segments. The beta subunit has a single transmembrane segment with most of its mass on the external surface of the membrane. The membrane topography of this class of pump was determined by a variety of methods prior to its confirmation by current images of two-dimensional crystals of the *Neurospora crassa* proton pump and the sarcoplasmic reticular Ca^{2+}-ATPase. Thus, tryptic digestion of cytoplasmic-side-out vesicles, *in vitro* and *in vivo* translation and labeling with sided reagents defined the 10 membrane segments, as illustrated in Fig. 2, as well as the single segment of the beta subunit.

Trypsinolysis followed by tricine gradient gel separation of the SDS-solubilized membrane fraction and sequencing provided details of the sequences of the first eight membrane segments, as did labeling either with thiophilic reagents such as omeprazole, lansoprazole or pantoprazole (M3/4, M5/6 and M7/8) or with photoaffinity derivatives of SCH 28080 (M1/2) (Besancon et al., 1997; Munson et al., 1991). *In vitro* transcription/translation studies of the 10 hydrophobic sequences provided evidence for membrane insertion of M1/2, M3/4, M8 and M9/10, enabling a model with ten transmembrane segments to be proposed (Bamberg and Sachs, 1994). Although the number of transmembrane helices was obtained from such studies, their boundaries and arrangement were not.

When the membrane arrangements of P_1- and P_2-ATPases are compared, it is found that they share a seeming core structure, consisting of six membrane-inserted segments, where the second and third and fourth and fifth such segments of the P_2-ATPases are separated by large cytoplasmic sectors, and in particular, the fourth and fifth such segments bound the phosphorylation and ATP-binding domains. With this general analysis, the P_1-ATPases have two membrane-spanning sequences preceding the core structure of six membrane-spanning segments, whereas the P_2-ATPases have four membrane-spanning segments following the six-

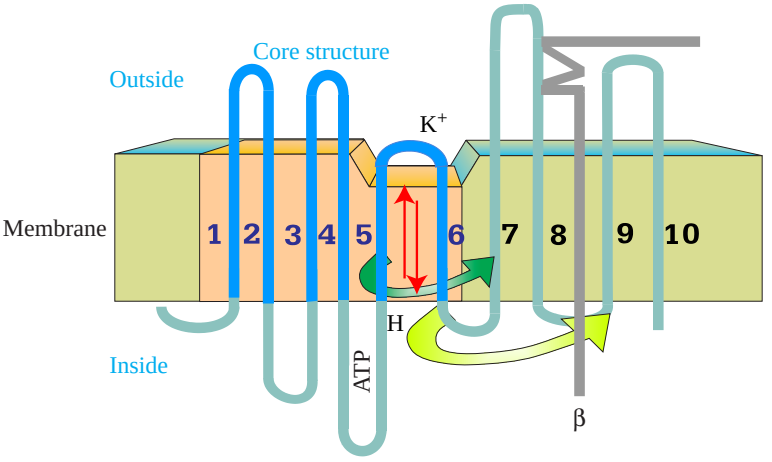

Fig. 2. A diagram illustrating the topography of the gastric (and other small-cation P_2-ATPases) in which the core structure consisting of the first six membrane-spanning segments is highlighted. The beta subunit (present in Na^+/K^+- and H^+/K^+-ATPases) is illustrated as associated with the beginning of the eighth membrane-spanning domain, as shown by wheat germ agglutinin (WGA) chromatography after trypsinization (Shin and Sachs, 1994), and the fifth and sixth pair of membrane-spanning segments also remains associated with membrane-spanning segments 7 and 8 provided that the linkage between segments 8 and 9 is not cleaved (Shin and Sachs, 1994), arguing for proximity of segments 5/6 and segments 9/10 in the membrane (curved arrow). This figure also shows the concept that membrane-spanning segments 5/6 interact more with other membrane-spanning segments than with phospholipid (white background).

transmembrane-segment core structure. The diagram in Fig. 2 shows the two-dimensional arrangement of the gastric ATPase.

Arrangement of the membrane domain

Interaction between the alpha and beta subunits

Both biochemical and molecular biological approaches have been used to show that a major region of interaction of the external sequence of the beta subunit is with a sequence of amino acids immediately preceding the outside face of M8, which interacts with two regions of the beta subunit. There are undoubtedly other regions of interaction, but these are perhaps too weak to be revealed by either wheat germ agglutinin (WGA) chromatography or yeast two-hybrid analysis.

After trypsinolysis of intact vesicles, in which the catalytic membrane-embedded segments are now present as pairs in the membrane fraction and the beta subunit is present as an N-terminal truncated fragment with the external domain virtually intact, WGA column chromatography is able to retain the beta fragment, because of its sugar residues, along with any associated alpha subunit fragment. Using this method, the M7–M8 pair was retained on the column after solubilization of the digest in non-ionic detergent (Shin and Sachs, 1994). When non-ionic detergent was applied before tryptic digestion, a region of the alpha subunit corresponding to M7 to the beginning of M8 was retained along with the beta subunit, between Leu855 and Arg922 (Melle-Milovanovic et al., 1998).

When the yeast two-hybrid system was applied, a region of interaction with the beta subunit was found in the alpha subunit, namely between Arg898 and Thr928, enclosed within the biochemically defined segment described above (Melle-Milovanovic et al., 1998). However, previous work, using resistance to tryptic digestion and ouabain binding, showed that a chimera of the Na^+/K^+-ATPase alpha subunit containing the region from Gln905 to Val930 of the rat gastric H^+/K^+-ATPase preferentially assembled with the beta subunit of H^+/K^+-ATPase (Wang et al., 1997). Therefore, a homologous 16-amino-acid-residue sequence of the alpha subunit of the two enzymes, from position 907 to position 922 in the H^+/K^+-ATPase and from position 894 to position 909 in the Na^+/K^+-ATPase, might be a point of stable contact with the beta subunit, while differences in the sequence in this region can account for selective assembly of the beta subunits with their alpha counterparts. The alignment of this region of the H^+/K^+ and Na/K-ATPases is shown in Table 1 and suggests that differences in this region, such as the smaller number or position of charged amino acids in the H^+/K^+-ATPase sequence, may account for the selective association of the two subunits.

Table 1. *Alignment of part of the alpha subunits of H^+/K^+-ATPase and Na^+/K^+-ATPase*

```
H+/K+   907–922: QDLQDSYGQEWTFGQR
                 -|- ||||| ||- ||
Na+,K+  894–909: NDVEDSYGQQWTYEQR
```

Two regions of interaction were found within the beta subunit, between Gln64 and Asn130, as well as the region enclosed by Ala156 and Arg188 (Melle-Milovanovic et al., 1998). Although disulfide bonds are present in the beta subunit, these are unlikely to be found in the intracellular yeast hybrid expression system and, since these are cytoplasmic proteins in yeast, N-linked sugars are also not implicated in these interactions. Mutational evidence in the Na^+/K^+-ATPase has also suggested interaction in the C-terminal domain of the alpha subunit (Lemas et al., 1992), where the hydrophobic amino acids were found to be essential for assembly.

These data suggest that the extracytoplasmic loop before M8 is responsible for the major interactions with the extracellular domain of the beta subunit. Since the transmembrane segment of the beta subunit ends at position 62, and position 64 is included in the interaction, it is very likely that the transmembrane domain of the beta subunit is adjacent to the beginning of M8 of the alpha subunit.

What is the function of the beta subunit? Such a subunit is evidently not essential for plasma membrane expression of P_2-type ATPases since the fungal proton pumps and plasma-membrane Ca^{2+} pumps have no such associated subunit. The beta subunit is essential for functional expression in transfected cells (Caplan and Gottardi, 1993), and *Xenopus laevis* oocyte translation data *in vivo* show a distinct effect of the presence of the beta subunit on the stability of the alpha subunit for both Na^+/K^+- and H^+/K^+-ATPases (Beguin et al., 1998; Beggah et al., 1999). However, some catalytic subunit is expressed in H^+/K^+ beta knockout mice, although no acid secretion can be detected (K. Scarff and van Driel, in preparation). The beta subunit is always expressed in association with a K^+ counter-transport ATPase and may be linked to fixation of the outside face of M8 to enable construction of the high-affinity form of the K^+ binding site.

Arrangement of the membrane helices of the alpha subunit

As mentioned above, P_1-ATPases have two preceding sequences before the common core structure with six membrane-spanning segments. P_2-ATPases have four membrane-embedded segments after the core structure of six membrane-embedded segments. This comparison suggests that segments M1–M6 are responsible for the rectangular central array seen in two-dimensional crystals of the H^+- and Ca^{2+}-ATPases and further suggests that the peripheral segments consist of M7/8 and M9/10 (Zhang et al., 1998; Auer et al., 1998). Which segment is which is problematic, since the relationship between the membrane helices and the cytoplasmic stalk region is difficult to discern at the current resolution of approximately 0.8 nm.

The difficulty in cross linking the membrane segments of these P_2-type ATPases by most reagents illustrates that the membrane segments are arranged in a compact form, preventing access of reagents to the interior of the membrane domain. Some interesting results have been obtained using metal ions such as Cu^{2+} or Fe^{3+}, but these studies have not produced data that allow full definition of the contact regions

of the membrane segments of this type of pump (Goldshleger and Karlish, 1997; Shimon et al., 1998). As for topography, many techniques will be required to define the nature and arrangement of membrane segments seen in low-resolution two- or three-dimensional crystals, as were used recently for bacterial rhodopsin (Unger et al., 1997; Kimura et al., 1997).

Translation of membrane segments

The P_2-ATPases have four N-terminal hydrophobic sequences followed by a large stretch of approximately 500 amino acid residues before the five or six hydrophobic sequences towards the C-terminal end of the catalytic subunit. The first four hydrophobic sequences are inserted sequentially as signal-anchor or stop-transfer sequences. In the case of the Na^+/K^+-, H^+/K^+- and endoplasmic reticulum Ca^{2+}-ATPases, membrane insertion of M5–M8, whether *in vitro* or in *Xenopus laevis*, is not necessarily sequential. For example, M5 and M6 and M7 and M8 become stably associated in the translation product only in the presence of beta translation for both the Na^+/K^+-ATPases (Beguin et al., 1998; Beggah et al., 1999). This would suggest a clustering of these four segments and insertion as a group into the translocon and thence into the membrane. In the case of the H^+/K^+-ATPase, M9 is a good signal anchor and M10 is a stop-transfer segment, and these segments are therefore added subsequent to assembly of the two clusters of four membrane-inserted segments (Bamberg and Sachs, 1994).

The membrane domain and stability of M5/6

In the case of the H^+/K^+-ATPase, some information can be gleaned from the results of WGA retention chromatography and from data determining release of membrane segments after gentle trypsinization of the cytoplasmic surface in the presence of K^+. The beta subunit associates with the WGA column and retains a 21 kDa fragment of the alpha subunit, which represents M7–M10, as well as a separate M5/6 fragment. With full digestion in the absence of K^+, the 21 kDa fragment is cleaved after M8 and, although M7/8 are retained on the WGA column, neither M9/10 nor M5/6 remain beta-associated. These data suggest that M5/6 are in proximity to M9/10 and are released from the association when M8 is separated from M9.

Additional information derives from attempts to reconstruct the membrane domain by *in vitro* or *in vivo* translation of truncated pump or from individual segments or pairs of segments. First, it was not possible *in vitro* to demonstrate membrane insertion of M5 or M6, or even that matter of M7 either as signal-anchor or stop-transfer sequences, whereas M1, M2, M3, M4 and M9 were signal-anchor sequences, and M8 and M10 were stop-transfer sequences. Assembly of this region of the pump under *in vivo* conditions in *Xenopus laevis* oocytes appeared to require co-translation of the beta subunit, as if interaction with the region before M8 stabilized this sector in the membrane. These data may be taken to mean that this region of the membrane sector is not in general interacting mainly with the hydrophobic core of the bilayer but rather with other peptide segments.

With digestion of the Na^+/K^+-ATPase by trypsin in the presence of K^+ followed by K^+ removal, M5/6 were released into the medium (Lutsenko et al., 1995). In further support of this hypothesis as applied to these P_2-ATPases, when gastric H^+/K^+-ATPase is digested with trypsin in the presence of K^+, M5, M6, M7 and M8 are found to remain associated with the membrane. With removal of K^+, first the M5/6 pair and then the M7/8 pair are found to be released from the membrane following low-concentration SDS treatment. This evidence suggests that the region of the enzyme involving these two pairs of transmembrane segments interacts with protein rather than with phospholipid. Since M5/6 contain several hydrophilic residues including three carboxylic acids found to be essential for enzyme activity and ion transport, it is tempting to speculate that the protein/protein interactions of this region reflect a possible mobility. This mobility may reflect a transport-related conformational change.

Peculiar, and still unexplained, is the finding that H9 and H10 are not found as digestion products of the ATPase in intact, cytoplasmic-side-out vesicles, whereas all the other pairs of membrane-spanning regions are. This observation raises the possibility of post-translational modification. This modification is not disulfide linkage or palmitoylation, but might be farnesylation or myristoylation since chemical reduction or esterolysis does not help find these two segments. Using the same techniques, these regions of the sarcoplasmic reticular Ca^{2+}-ATPase and the Na^+/K^+-ATPase are readily found.

In summary, a combination of results from trypsinolysis, labeling and *in vitro* translation suggests an arrangement with 10 membrane-embedded segments for the catalytic subunit and a single such segment for the beta subunit, and these arrangements are consistent with the two-dimensional reconstructions shown thus far for P_2-type ATPases.

Inhibitor binding sites

To explore in more detail the possible arrangement of the 10 transmembrane segments of the H^+/K^+-ATPase, the binding sites of two classes of inhibitor were explored. One class of inhibitor, the substituted pyridyl methylsulfinyl benzimidazoles, are acid-activated thiophilic compounds that form stable disulfide bridges with cysteines accessible from the luminal or acidic surface of the pump. These compounds, such as omeprazole, are covalent inhibitors of the pump, and many are in use for treatment of acid-related diseases (Sachs et al., 1993). The second class is exemplified by 1,2α-imidazopyridines. These are strictly K^+-competitive (and therefore reversible) faster-acting inhibitors of gastric acid secretion also binding to the outside of the pump (Mendlein and Sachs, 1990). The gastric ATPase is unique among the P-ATPases in having two classes of low-molecular-mass, specific inhibitors. These can be used to define membrane segments and, by mutational analysis, can act as measuring devices for distances between membrane helices.

Reaction with cationic thiophilic reagents. The set of reactions that occurs with *in vivo* administration of these compounds, the benzimidazoles, when they are added to acid-

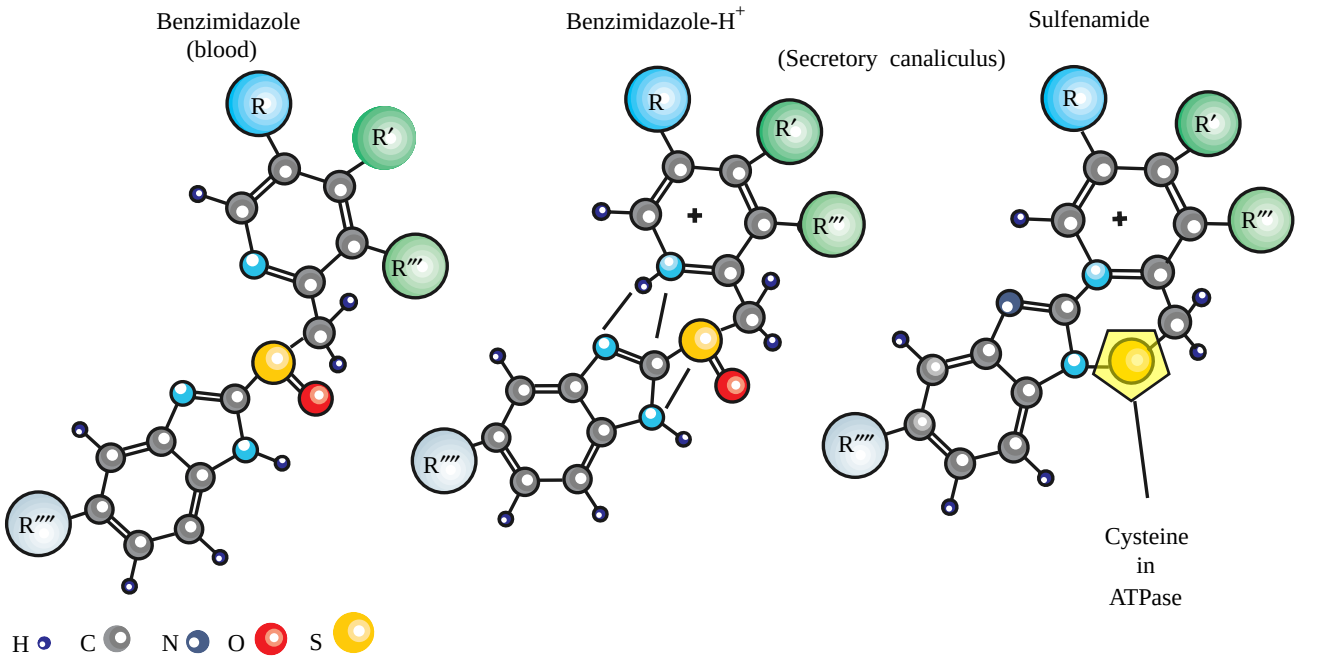

Fig. 3. The steps (protonation and acid-catalyzed conversion to sulfenamide) in the generation of the sulfhydryl-reactive sulfenamide from benzimidazole, which then reacts with cysteines accessible from the luminal surface of the H^+/K^+-ATPase.

transporting gastric ATPase vesicles involves first protonation in the acid space of the vesicle or the parietal cell, with accumulation therefore being dependent on the pKa of the weak base, usually set between 4.0 and 5.0. Following this accumulation in the acid space, there is acid-catalyzed conversion to a thiophilic reactive sulfenamide. The sulfenamide is then able to react with accessible cysteines of the H^+/K^+-ATPase. Several of these are predicted from the secondary structure, at positions 321, 813, 822, 892, 927 and 981 in the hog gastric H^+/K^+-ATPase sequence, with the N-terminal amino acid being glycine. The reaction pathway is illustrated in Fig. 3.

When [^{3}H]omeprazole is added to vesicles under acid-transport conditions, there is covalent, reducing-agent-reversible, labeling of the catalytic subunit of the ATPase. Following trypsinization, SDS solubilization, labeling with fluorescein-5-maleimide (FMI) and tricine gradient gel electrophoresis, all the radioactivity is associated with a band with a sequence corresponding to M5/6. The degree of inhibition corresponds to labeling of this region. Two cysteines are present in this membrane pair, at positions 813 and 822. All the radioactivity is associated with this band. When this band is isolated from the gel and re-electrophoresed (Fig. 4), most of the radioactivity is associated with the FMI-labeled band. When this band is digested with thermolysin and again separated by SDS gel

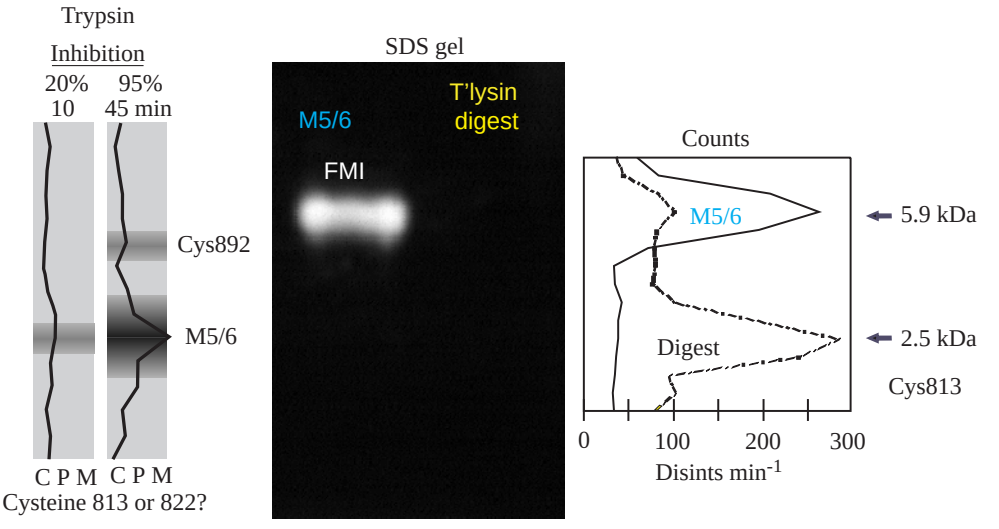

Fig. 4. Identification of the inhibitory site of omeprazole. On the left is the labeling of M5/6 correlating with inhibition, with minor labeling of Cys892 in M7/8. With this M5/6 band cut out and labeled with fluorescein-5-maleimide (FMI) and run again on SDS–PAGE, the center panel shows that fluorescence and the label are exclusively associated with the fluorescent band. After thermolysin (T'lysin) digestion, all the counts are retained in a 2.5 kDa fragment (which cannot include Cys822), showing that labeling and inhibition by omeprazole are determined by covalent reaction with Cys813. M, membrane-spanning segment of the ATPase.

electrophoresis, all the counts are present in a band whose sequence begins with the same N-terminal sequence as M5/6, but cannot, on the basis of molecular mass, include Cys822. The FMI fluorescence has disappeared. Hence, labeling and inhibition correlate with disulfide formation at Cys813 (Besancon et al., 1997). Another compound, pantoprazole, appears to label both cysteines, suggesting access to both of these residues by a cationic, relatively hydrophilic molecule (Shin et al., 1993).

From this result, Cys813 is readily accessible from the luminal surface, as is Cys892. Another cysteine that is labeled by lansoprazole is Cys321 at the end of M3. Cys813 follows a PLPL turn at the end of M5 and is therefore in the loop between M5 and M6 or at the beginning of M6. The M5/6 pair of cysteines is the pair defined as flexible by the extraction and translation data discussed above. Of interest when inhibition by imidazo-pyridines is considered is that binding of the reversible inhibitor SCH 28080 prevents inhibition by the covalent inhibitor omeprazole (Hersey et al., 1988). This interaction suggests that there is some overlap of binding sites for these two inhibitors. Other benzimidazoles are able to bind to Cys321 and even Cys822. In expression studies using an alpha/beta fusion protein, mutation of Cys822 resulted in insensitivity to inhibition of Rb^+ transport by omeprazole in these HEK 293 cells, whereas mutation of Cys813, surprisingly, was without effect except that omeprazole inhibition now appeared to be reversible (Lambrecht et al., 1998). We interpreted these data as showing a reversible binding domain in the vicinity of Cys822 and a covalent binding domain at Cys813, which would make the connecting loop between M5 and M6 longer than usually stated.

Reaction with 1,2α-imidazo-pyridines. The likely three-dimensional structure of the imidazo-pyridine inhibitors of the H^+/K^+-ATPase has been determined by synthesising a variety of analogs, and the fused ring, illustrated in Fig. 5, is the paradigm for this type of inhibitor, with the benzene ring orthogonal to the planar fused ring structure. The size of this molecule at its widest point is approximately 1.2 nm, compared with 1.4 nm for the largest of the benzimidazoles. The compounds have a tail region (the benzene ring) and a head region that consists of the protonated pyridine, which is considered to be the active form. These compounds provide a unique opportunity for analysis of a P_2-type pump, using an inhibitor small enough to penetrate the membrane domain. Both ouabain and thapsigargin are too large for this type of analysis to be applied to the Na^+/K^+ and sarcoplasmic reticular Ca^{2+}-ATPases.

Two approaches were taken to determine the binding sites for a reversible inhibitor. The first was to generate a photoaffinity probe of a radioactive derivative of SCH 28080, as illustrated in Fig. 5. Reaction displaced by K^+ was found to be exclusively within the M1/2 region of the enzyme (Munson et al., 1991). However, the linkage was acid-unstable, and the amino acid labeled by the reagent could not therefore be defined. Also, the nitrene was generated in the tail of the compound, perhaps therefore not defining the K^+-competitive region of binding.

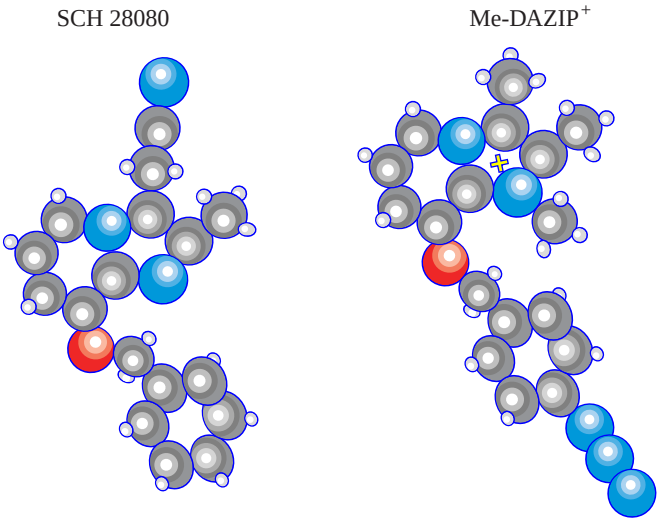

Fig. 5. The structure of unprotonated SCH 28080 and the cationic photoaffinity derivative [^{3}H]Me-DAZIP.

The second approach was to generate site-directed mutations and determine changes in affinity for the imidazopyridines and the competing ion, K^+, or its surrogate NH_4^+. The wild-type rabbit gastric pump and its mutants are expressed in HEK 293 cells as heterodimers by using a stable cell line expressing the rabbit beta subunit with selection by (K. Munson, N. Lambrecht and G. Sachs, in preparation) and transfection with the rabbit alpha subunit using zeocin as a selection marker. Using this dual-selection transfection method, activities of up to $3\,\mu mol\,mg^{-1}$ total membrane protein h^{-1} are routinely measured. This activity is sufficient to provide adequate kinetic data. The specific activity of the wild type and of most of the mutants is close to that of hog gastric ATPase, namely around $100\,\mu mol\,mg^{-1}\,h^{-1}$. With such activities, the measurement of K_m for NH_4^+, the cation used to obviate problems of vesicles of limited permeability and of K_i for SCH 28080 is accurate and reproducible. Mutations performed thus far can be classified, in terms of effect on K_i, into those with no effect on K_i, those with a minor effect, those with an intermediate effect and those with major effects. If these have little or no effect on K_m and retain competitive kinetics, it can be assumed that these are selective for SCH 28080 binding and do not have general conformational effects.

Since SCH 28080 has no effect on the Na^+/K^+-ATPase, many of the mutations were chosen on the basis of divergence between the Na^+/K^+- and H^+/K^+-ATPase membrane sequences. These studies are still incomplete, but a picture is starting to emerge of the topography of the core structure with six membrane-embedded segments, showing a vestibule containing the SCH 28080 binding site that does not overlap with the cation binding site but does overlap with the omeprazole binding site at Cys813.

Three mutations have been carried out in M1 and M2, Met113 to Leu, Ile119 to Leu and Leu121 to Phe. Of these, the

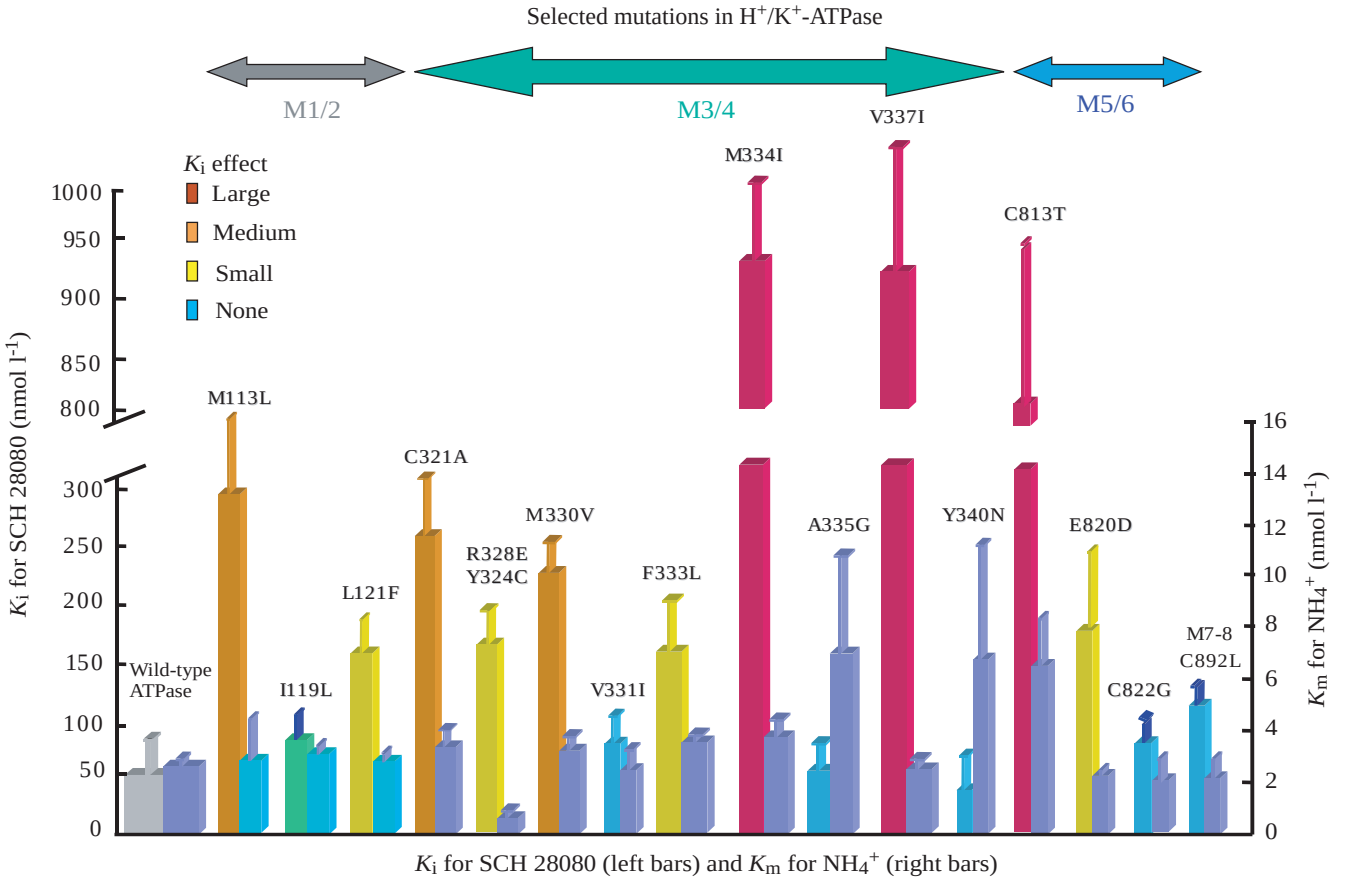

Fig. 6. A summary of the effects of site-directed mutations in the core structure of the H^+/K^+-ATPase on the kinetics of NH_4^+ activation and SCH 28080 inhibition. The color coding corresponds to the size of the effect on K_i. The left-hand of each pair of columns refers to the apparent inhibitor constant (K_i), and the right-hand of each pair (dark blue) refers to the apparent Michaelis constant (K_m). Data from N. Lambrecht, K. Munson, O. Vagina and G. Sachs, in preparation; K. Munson, N. Lambrecht and G. Sachs, in preparation. Values are means + S.E.M., N=12. M, membrane-spanning segment of the ATPase.

Met113 to Leu mutation had a large effect on the K_i, the Leu121 to Phe mutation a minor effect and the Ile119 to Leu mutation no effect (Fig. 6). Met113 is therefore likely to be the amino acid to which the photoaffinity derivative was bound, especially since the methylene group would be highly reactive with the nitrene generated upon photolysis.

In M3 and M4, the mutation of Cys321 to Ala results in a moderate increase in the K_i for SCH 28080. This is predicted to be at the outside edge of M3 and is a cysteine that is accessible to lansoprazole, a benzimidazole-type of enzyme inhibitor. This particular mutation affects the K_m for NH_4^+, and inhibition becomes mixed, suggesting a conformational change also affecting SCH 28080 binding (N. Lambrecht, K. Munson, O. Vagina and G. Sachs, in preparation).

Mutations in M4 in the amino acids distinct from those of the Na^+/K^+-ATPase towards the outside of this segment have, in general, significant effects on the affinity of SCH 28080; those towards the inside have no effect on SCH 28080 kinetics but large effects on ATPase activity. Thus, the mutation Met334 to Ileu and of Val337 to Ileu have large effects on SCH 28080 affinity, but are notably without effect on the affinity for NH_4^+. The mutation Phe333 to Leu also reduces SCH 28080 affinity, but less so, while the mutation Met330 to Val has a minor effect. These amino acids are on one side of the helix, and this surface of M4 is postulated to bind SCH 28080 (Lambrecht et al., 1998).

None of these mutations affected NH_4^+ affinity, but Ala335 to Gly and Tyr340 to Asn reduced NH_4^+ affinity and also had a major effect on enzyme activity. Tyr 340 has been implicated in the targeting of the H^+/K^+-ATPase to the apical membrane of cultured cells (K. Munson, N. Lambrecht and G. Sachs, in preparation) and is on a different surface of the M4 helix. Perhaps this region of the helix is implicated in ion binding.

The M4 segment of the enzyme is therefore of importance in determining SCH 28080 affinity. The mutations made were in residues conserved between the Na^+/K^+- and H^+/K^+-ATPases and hence responsible, at least in part, for the discrimination of SCH 28080 by the H^+/K^+-ATPase. The loss of SCH 28080 affinity with no effects on the affinity of the competitive cation therefore argues that the outer region of M4, although binding the competitive inhibitor, is not involved in binding the counter-transported ion. However, when the ion is

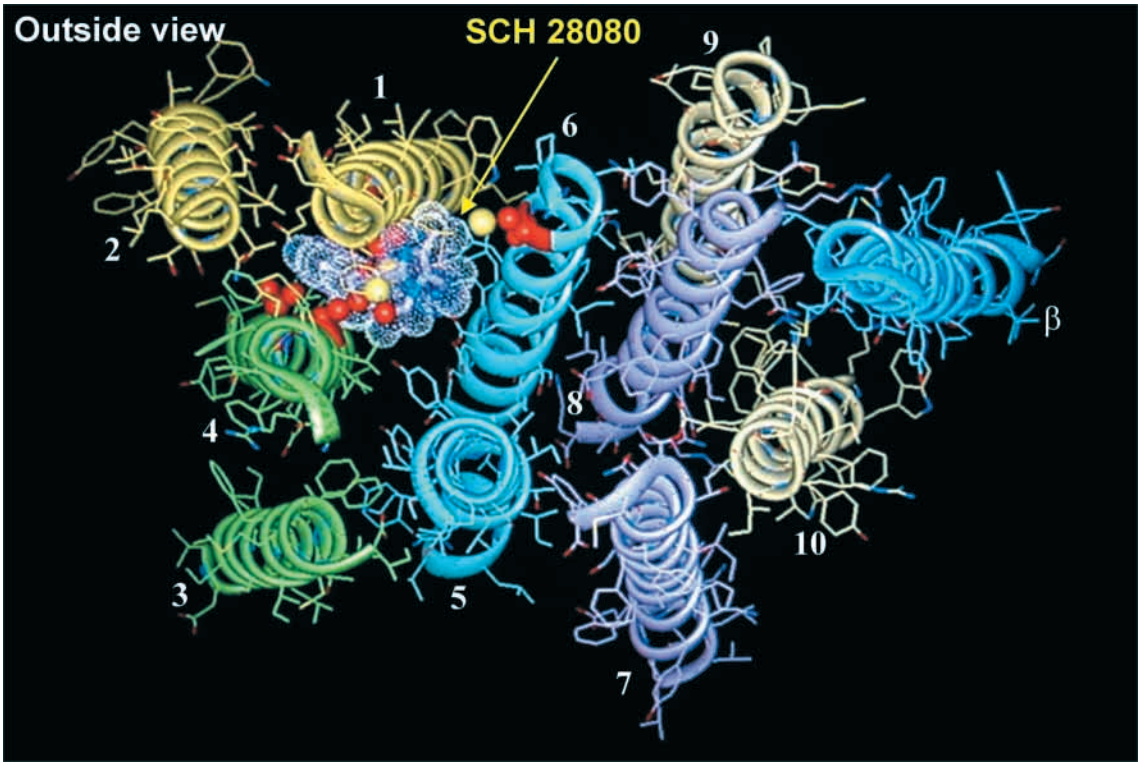

Fig. 7. A molecular model prepared using Biosym software and helix/helix interaction minimization protocols illustrating the placement of amino acids (1–10) mutated in an exploration of the binding region of SCH 28080 (SCH), with a tentative alignment with helices illustrated for the core structure of the H^+-ATPase of *Neurospora crassa* and the sarcoplasmic reticular Ca^{2+}-ATPase. M1–M6, membrane spanning segments 1–6; K_i, apparent inhibitor constant. Two different views are shown.

bound, SCH 28080 cannot bind, indicating a change in this region induced by NH_4^+ (or K^+) binding.

In M5 and M6, the mutation Cys813 to Thr markedly reduces SCH 28080 affinity (increases K_i), whereas the mutation Glu820 to Asp has a moderate effect. The former has a minor effect on the affinity for NH_4^+, the latter none. The mutation Cys822 to Gly is without effect on either SCH 28080 affinity or NH_4^+ kinetics. These data are summarized in Fig. 6 (N. Lambrecht, K. Munson, O. Vagina and G. Sachs, in preparation; Lambrecht et al., 1998).

In M7 and M8, a single mutation was carried out on the cysteine slowly labeled by omeprazole, Cys892 to Leu. No kinetic effect was observed (Lambrecht et al., 1998).

The analysis of the results of these mutations places the binding region of SCH 28080 within the core segments of the membrane domain of the H^+/K^+-ATPase, but molecular modeling shows the presence of a vestibule necessary to accommodate these results. Evidently, the surface of M4 from Met330 to Val337 is a major binding region for this K^+-competitive inhibitor; Met113 towards the middle of M1 and Cys813 (the site of covalent binding of omeprazole and other benzimidazoles) at the end of M5 or the beginning of M6 must be included in this region. These positions must be within 1.2 nm of each other given the size of SCH 28080. The effects of Cys321 mutations on folding and kinetics suggest a more general effect.

A working *ab initio* model of this region of the pump, as illustrated in Fig. 7, can be further modified by using the tilt angles visualized in the reconstruction of the H^+-ATPase of *Neurospora crassa* and the sarcoplasmic reticular Ca^{2+}-ATPase and the helices external to the core added from the proximity of M5/6 and M9/10 and the length of the loop between M7/8. This model predicts which other amino acids should be mutated for a further detailed analysis of SCH 28080 kinetics. Both the above results and the model also predict an overlap between SCH 28080 binding and omeprazole binding, providing a rationale for the older finding that binding of the imidazo-pyridine prevents covalent binding by omeprazole, even in the presence of the luminal acidity generated in acid-transporting conditions (Hersey et al., 1988).

References

Auer, M., Scarborough, G. A. and Kuhlbrandt, W. (1998). Three-dimensional map of the plasma membrane H^+-ATPase in the open conformation. *Nature* **392**, 840–843.

Bamberg, K. and Sachs, G. (1994). Topological analysis of H^+,K^+-ATPase using *in vitro* translation. *J. Biol. Chem.* **269**, 16909–16919.

Bayle, D., Wangler, S., Weitzenegger, T., Steinhilber, W., Volz, J., Przybylski, M., Schafer, K. P., Sachs, G. and Melchers, K. (1998). Properties of the P-type ATPases encoded by the copAP

operons of *Helicobacter pylori* and *Helicobacter felis*. *J. Bacteriol.* **180**, 317–329.

Beauge, L. A. and Glynn, I. M. (1979). Occlusion of K ions in the unphosphorylated sodium pump. *Nature* **280**, 510–512.

Beggah, A. T., Beguin, P., Bamberg, K., Sachs, G. and Geering, K. (1999). Beta-subunit assembly is essential for the correct packing and the stable membrane insertion of the H,K-ATPase alpha-subunit. *J. Biol. Chem.* **274**, 8217–8223.

Beguin, P., Hasler, U., Beggah, A., Horisberger, J. D. and Geering, K. (1998). Membrane integration of Na,K-ATPase alpha-subunits and beta-subunit assembly. *J. Biol. Chem.* **273**, 24921–24931.

Besancon, M., Simon, A., Sachs, G. and Shin, J. M. (1997). Sites of reaction of the gastric H,K-ATPase with extracytoplasmic thiol reagents. *J. Biol. Chem.* **272**, 22438–22446.

Caplan, M. J. and Gottardi, C. J. (1993). Molecular requirements for cell surface expression of multi-subunit ion-transporting ATPases. *J. Biol. Chem.* **268**, 24921–24931.

Chow, D. C., Browning, C. M. and Forte, J. G. (1992). Gastric H^+-K^+-ATPase activity is inhibited by reduction of disulfide bonds in beta-subunit. *Am. J. Physiol.* **263**, C39–C46.

Esmann, M. (1985). Occlusion of Rb^+ by detergent-solubilized (Na^++K^+)-ATPase from shark salt glands. *Biochim. Biophys. Acta* **815**, 196–202.

Forte, J. G., Ganser, A. L. and Tanisawa, A. S. (1974). The K^+-stimulated ATPase system of microsomal membranes from gastric oxyntic cells. *Ann. N.Y. Acad. Sci.* **242**, 255–267.

Gassel, M., Siebers, A., Epstein, W. and Altendorf, K. (1998). Assembly of the Kdp complex, the multi-subunit K^+-transport ATPase of *Escherichia coli*. *Biochim. Biophys. Acta* **19995**, 77–84.

Geering, K. (1991). The functional role of the beta-subunit in the maturation and intracellular transport of Na,K-ATPase. *FEBS Lett.* **285**, 189–193.

Goldshleger, R. and Karlish, S. J. D. (1997). Fe-catalyzed cleavage of the alpha subunit of Na/K-ATPase: Evidence for conformation-sensitive interactions between cytoplasmic domains. *Proc. Natl. Acad. Sci. USA* **94**, 9596–9601.

Hasler, U., Wang, X., Crambert, G., Beguin, P., Jaisser, F., Horisberger, J. D. and Geering, K. (1998). Role of beta-subunit domains in the assembly, stable expression, intracellular routing and functional properties of Na,K-ATPase. *J. Biol. Chem.* **273**, 30826–30835.

Hersey, S. J., Steiner, L., Mendlein, J., Rabon, E. and Sachs, G. (1988). SCH28080 prevents omeprazole inhibition of the gastric H^+/K^+-ATPase. *Biochim. Biophys. Acta* **956**, 49–57.

Kimura, Y., Vassylyev, D. G., Miyazawa, A., Kidera, A., Matsushima, M., Mitsuoka, K., Murata, K., Hirai, T. and Fujiyoshi, Y. (1997). Surface of bacteriorhodopsin revealed by high-resolution electron crystallography. *Nature* **389**, 206–211.

Lambrecht, N., Corbett, Z., Bayle, D., Karlish, S. J. and Sachs, G. (1998). Identification of the site of inhibition by omeprazole of an alpha–beta fusion protein of the H,K-ATPase using site-directed mutagenesis. *J. Biol. Chem.* **273**, 13719–13728.

Lemas, M. V., Takeyasu, K. and Fambrough, D. M. (1992). The carboxyl-terminal 161 amino acids of the Na,K-ATPase alpha-subunit are sufficient for assembly with the beta-subunit. *J. Biol. Chem.* **267**, 20987–20991.

Lutsenko, S., Anderko, R. and Kaplan, J. H. (1995). Membrane disposition of the M5–M6 hairpin of Na^+,$K(^+)$-ATPase alpha subunit is ligand dependent. *Proc. Natl. Acad. Sci. USA* **92**, 7936–7940.

Melchers, K., Weitzenegger, T., Buhmann, A., Steinhilber, W., Sachs, G. and Schafer, K. P. (1996). Cloning and membrane topology of a P type ATPase from *Helicobacter pylori*. *J. Biol. Chem.* **271**, 446–457.

Melle-Milovanovic, D., Milovanovic, M., Nagpal, S., Sachs, G. and Shin, J. M. (1998). Regions of association between the alpha and the beta subunit of the gastric H,K-ATPase. *J. Biol. Chem.* **273**, 11075–11081.

Mendlein, J. and Sachs, G. (1990). Interaction of a K^+-competitive inhibitor, a substituted imidazo[1,2αd] pyridine, with the phospho- and dephosphoenzyme forms of H^+,K^+-ATPase. *J. Biol. Chem.* **265**, 5030–5036.

Munson, K. B., Gutierrez, C., Balaji, V. N., Ramnarayan, K. and Sachs, G. (1991). Identification of an extracytoplasmic region of H^+,K^+-ATPase labeled by a K^+-competitive photoaffinity inhibitor. *J. Biol. Chem.* **266**, 18976–18988.

Polvani, C., Sachs, G. and Blostein, R. (1989). Sodium ions as substitutes for protons in the gastric H,K-ATPase. *J. Biol. Chem.* **264**, 17854–17859.

Rabon, E. C., Smillie, K., Seru, V. and Rabon, R. (1993). Rubidium occlusion within tryptic peptides of the H,K-ATPase. *J. Biol. Chem.* **268**, 8012–8018.

Sachs, G. (1998). Symposium on ion motive ATPases. *Acta Physiol. Scand.* **643** (Suppl.), 5–6.

Sachs, G., Chang, H. H., Rabon, E., Schackman, R., Lewin, M. and Saccomani, G. (1976). A nonelectrogenic H^+ pump in plasma membranes of hog stomach. *J. Biol. Chem.* **251**, 7690–7698.

Sachs, G., Shin, J. M., Besancon, M. and Prinz, C. (1993). The continuing development of gastric acid pump inhibitors. *Aliment. Pharmac. Ther.* **7** (Suppl.), 4–12 (discussion pp. 29–31).

Serrano, R. (1988). Structure and function of proton translocating ATPase in plasma membranes of plants and fungi. *Biochim. Biophys. Acta* **947**, 1–28.

Shimon, M. B., Goldshleger, R. and Karlish, S. J. D. (1998). Specific Cu^{2+}-catalyzed oxidative cleavage of Na,K-ATPase at the extracellular surface. *J. Biol. Chem.* **273**, 34190–34195.

Shin, J. M., Besancon, M., Simon, A. and Sachs, G. (1993). The site of action of pantoprazole in the gastric H^+/K^+-ATPase. *Biochim. Biophys. Acta* **1148**, 223–233.

Shin, J. M. and Sachs, G. (1994). Identification of a region of the H,K-ATPase alpha subunit associated with the beta subunit. *J. Biol. Chem.* **269**, 8642–8646.

Unger, V. M., Hargrave, P. A., Baldwin, J. M. and Schertler, G. F. X. (1997). Arrangement of rhodopsin transmembrane alpha-helices. *Nature* **389**, 203–206.

Vilsen, B. and Andersen, J. P. (1986). Occlusion of Ca^{2+} in soluble monomeric sarcoplasmic reticular Ca^{2+}-ATPase. *Biochim. Biophys. Acta* **855**, 429–431.

Walderhaug, M. O., Post, R. L., Saccomani, G., Leonard, R. T. and Briskin, D. P. (1985). Structural relatedness of three ion-transport adenosine triphosphatases around their active sites of phosphorylation. *J. Biol. Chem.* **260**, 3852–3859.

Wang, S. G., Eakle, K. A., Levenson, R. and Farley, R. A. (1997). Na^+-K^+-ATPase alpha-subunit containing Q905–V930 of gastric H^+-K^+-ATPase alpha preferentially assembles with H^+-K^+-ATPase beta. *Am. J. Physiol.* **272**, C923–C930.

Zhang, P., Toyoshima, C., Yonekura, K., Green, N. M. and Stokes, D. (1998). Structure of the calcium pump from sarcoplasmic reticular at 8-Å resolution. *Nature* **392**, 835–839.